

Molecular Physics

An International Journal at the Interface Between Chemistry and Physics

ISSN: 0026-8976 (Print) 1362-3028 (Online) Journal homepage: <http://www.tandfonline.com/loi/tmph20>

The effect of ionisation of silica nanoparticles on their binding to nonionic surfactants in oil–water system: an atomistic molecular dynamic study

Parul Katiyar & Jayant K. Singh

To cite this article: Parul Katiyar & Jayant K. Singh (2018): The effect of ionisation of silica nanoparticles on their binding to nonionic surfactants in oil–water system: an atomistic molecular dynamic study, Molecular Physics, DOI: [10.1080/00268976.2018.1456683](https://doi.org/10.1080/00268976.2018.1456683)

To link to this article: <https://doi.org/10.1080/00268976.2018.1456683>



Published online: 18 Apr 2018.



Submit your article to this journal [↗](#)



View related articles [↗](#)



View Crossmark data [↗](#)

The effect of ionisation of silica nanoparticles on their binding to nonionic surfactants in oil–water system: an atomistic molecular dynamic study

Parul Katiyar and Jayant K. Singh

Department of Chemical Engineering, Indian Institute of Technology Kanpur, Kanpur, India

ABSTRACT

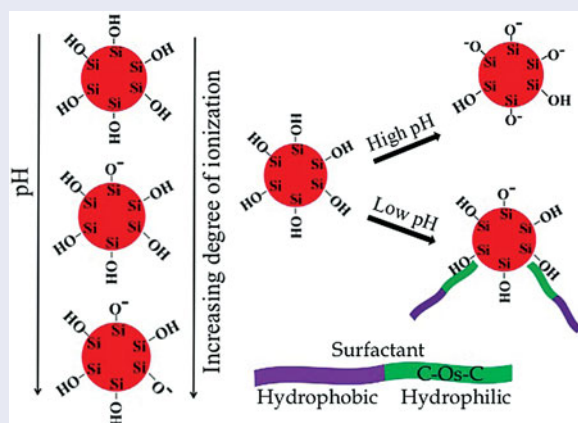
In this study, the adsorption of nonionic surfactant, triethylene glycol monododecyl ether ($C_{12}E_3$), on a surface of silica nanoparticle (NP) has been studied with variation in the degree of ionisation (DI) of silica NP using all-atom molecular dynamic simulations in hexadecane–water system. Hydrogen bonding is found to be responsible for the adsorption of $C_{12}E_3$ on NP, particularly at low DI. We observe that with increasing DI of NP, the amount of adsorption of $C_{12}E_3$ on NP reduces, which is negligible beyond DI ~ 0.5 . The decrease in the adsorption with increasing DI is due to the decrease in the number of hydrogen bonds formed by the silica NP with surfactant molecules. Potential of mean force (PMF) profiles indicate attractive interactions between NP and $C_{12}E_3$ for DI < 0.5 , and for larger DI depletion effect is observed. This work explains the unusual effect of nonionic surfactant on interfacial tension in the presence of silica particles as observed in recent experiments.

ARTICLE HISTORY

Received 25 December 2017
Accepted 14 March 2018

KEYWORDS

Interfacial tension; nonionic surfactant; molecular dynamics; silica nanoparticles



1. Introduction

The adsorption of surfactant at interfaces is a complex phenomenon and plays an important role in many industrial and daily life applications [1–3] such as enhanced oil recovery [4], mineral flotation, nanolithography [5], cosmetics and emulsions [6]. The adsorption studies of ionic [7] and nonionic [8–10] surfactants and their mixtures [2,5] on silica are useful in several applications for example, detergency, enhanced oil recovery, surface modification and pickering emulsions. Silica has been studied extensively, as it is an important component of various products such as glass, paints, ceramics, plastics, rubber, etc. and is also abundantly available in nature [7]. Various different ionic surfactants have been extensively studied in the presence of silica [3,7,11] and

their behaviour is well understood. On the other hand, the behaviour of nonionic surfactant in the presence of silica nanoparticles (NPs) is intriguing and not well understood.

Partyka *et al.* [9] studied the effect of concentration, temperature, salt and molecular structure of the nonionic surfactants on its adsorption on silica gel. Boomgard *et al.* [12] measured the adsorption of nonionic surfactant on silica and polystyrene particles and found that the weight adsorbed per unit area decreases with the increase in polyethylene oxide chain length. The adsorption amount was also observed to increase with temperature. Somasundaran *et al.* [10] studied the effect of degree of ethoxylation of long chain alcohols on their adsorption on silica.

The authors have mentioned hydrogen bonding as the initial reason for adsorption of ethoxylated alcohols. Denoyl *et al.* [13] have studied the adsorption of nonionic (Triton series) and anionic surfactants on silica, alumina and kaolin surfaces. They found that the adsorption of nonionic surfactant increases with the decrease in pH of the solution. Thibaut *et al.* [2] studied the adsorption of a mixture of sodium dodecyl sulfate (SDS) and pentaethylene glycol monododecyl ether ($C_{10}E_5$) on silica surface and found that addition of SDS decreases the amount of adsorption of $C_{10}E_5$ due to the formation of mixed micelles in the solution. The adsorption of polyethylene oxide [14] and different nonionic surfactants such as nonaethylene glycol dodecyl ether ($C_{12}E_9$) [8], hexaethylene glycol monotetradecyl ether ($C_{14}E_6$), octaethylene glycol monohexadecyl ether ($C_{16}E_8$) [15], hexaethylene glycol monododecyl ether ($C_{12}E_6$) [1] and pentaethylene glycol monododecyl ether ($C_{12}E_5$) [16] on silica surface have also been studied. The adsorption of $C_{12}E_5$ on the silica NPs of different sizes increases with the increase in NP size [16]. Few works have also been done where the structure formed by the adsorbed nonionic surfactants on silica NPs is observed. Cummins *et al.* [17] and Penfold *et al.* [18] have studied the nature of the adsorption of various different alkyl polyoxyethylene ether surfactants on silica sol and have investigated the effect of surfactant concentration, surfactant type and temperature. The structure of adsorbed TX-100 on colloidal silica in water has also been investigated by Despert *et al.* [19]. The self-assembled structure formed by two different nonionic surfactants $C_{12}E_5$ and n-dodecyl- β -maltoside in the presence of silica sol of single particle size [20], and nonionic surfactants dimethyldodecylamine-*N*-oxide and pentaethylene glycol monododecyl ether for different NPs size is studied in H_2O/D_2O solvent mixture by Lugo *et al.* [21].

Several review works have also focused on summarising the surfactant adsorption at the solid–water interface [5,22]. Almost all the studies listed above are based on the adsorption of nonionic surfactants on a solid surface in the presence of water. On the other hand, very few studies are reported on the adsorption of nonionic surfactant on silica NPs in oil–water systems.

The genesis of this work stems from our previous study [23] and several other studies [24–26], where varying behaviour of interfacial tension (IFT) was observed for the oil–water system having nonionic surfactants, with the addition of silica NPs. We noticed that in some studies increase in IFT is reported with the addition of silica NPs to the oil–water system containing nonionic surfactant [24,25], while few studies report no change [26]. At a pH of 10, Ma *et al.* [26] observed no change in IFT with the addition of negatively charged

silica NPs to the trichloroethylene–water system containing nonionic (Triton X-100, C_8E_4 , $C_{12}E_4$, $C_{14}E_4$) surfactants. This behaviour is attributed to the weak affinity between the nonionic surfactant and the NPs at the specified pH. However, a similar study at a pH of 2 is reported by Pichot *et al.* [25], where addition of silica NPs is found to increase the IFT of the oil–water system having a low concentration of nonionic surfactants (Tween 60 and sodium caseinate). The variation in the IFT behaviour is attributed to the difference in the pH maintained during the study. In a recent work, Biswal *et al.* [24] also observed an increase in IFT on the addition of $SiO_2/ ZnO/ TiO_2$ NPs to *n*-hexane/*n*-heptane/*n*-decane/toluene–water systems, having nonionic surfactants (Triton X-100 and Tween 20). The authors [24] postulated adsorption of surfactant on NPs as one of the reasons for the increase in IFT. In our recent work [23] we have showed that the adsorption of nonionic surfactant on silica NPs leads to an increase in IFT, however when the surfactant does not adsorb on the NP there is no change in the IFT as compared to oil–water surfactant IFT. Nevertheless, the change in the adsorption behaviour with the pH is still not well understood.

Role of pH lies mainly in ionising the molecule if the molecule is ionisable. Burcik *et al.* [27] in 1951 studied the effect of pH on surface tension. They found that the hydrolysable surfactants have an effect on surface tension with the change in pH, while the surfactants that do not hydrolyse have no effect of the changing pH of the solution. Furthermore, when a pH is maintained using ionisable molecules then the amount of molecules is responsible for the change in surface tension and not the pH value. For example, when acetic acid and citric acid are used to maintain a fixed pH the surface tension of water is observed to reduce more for acetic acid as compared to citric acid because more amount of acetic acid is required to maintain the same pH [28]. In a study of the effect of graphene oxide (GO) on the oil–water system, it was shown that the IFT value of oil–water decreases with decrease in pH because the GO becomes less hydrophilic and moves to the oil–water interface than being in water [29]. On the other hand, it is shown that surface tension of water in the presence of surface-active agents, which do not hydrolyse, is independent of pH [27].

Nevertheless, the change in adsorption behaviour of nonionic surfactant with the pH is not well reported for oil–water interface systems, particularly using molecular simulations. The main objective of this study is to understand the change in adsorption of nonionic surfactant on silica NPs in the oil–water system with varying degree of ionisation (DI) (due to changes in pH) of silica NPs using all-atom molecular dynamics simulations. In order to get a clear understanding of the effect of pH,

we have performed atomistic molecular dynamic simulations to study the effect of changing DI of silica NPs. In Section 2 we have discussed the model and details of the simulations. Section 3 presents the results and discussions and finally conclusions are given in Section 4.

2. Model and methodology

Molecular dynamic simulations are performed for hexadecane–water system containing one silica NP of 3 nm diameter and 100 chains of nonionic surfactant, $C_{12}E_3$. Water is modelled using SPC/E (extended simple point charge) [30] potential. Hexadecane is based on the model of Boland *et al.* [31]. The force field parameters for surfactant $C_{12}E_3$ are taken from the work of Shi *et al.* [32] and the silica NP is modelled based on the force field of Emami *et al.* [33]. Silica NP is made by cutting a sphere from the crystal lattice of cristoballite. Unsaturated silicon atoms are removed from the sphere (nanoparticle) surface and the nonbridging oxygen atoms are saturated with hydrogen atoms yielding hydroxyl group [34]. Silica NPs are ionised to different degree by removing H atom from the O–H bonds of surface silanol groups (–SiOH). The different DI corresponds to different number of O–H bonds being broken. The removed H atoms of the O–H bond are replaced by sodium ions (Na^+) in the system to maintain a net zero charge.

The interaction energy between two atoms is expressed as a sum of bonded and nonbonded terms. The nonbonded interaction includes Lennard-Jones and electrostatic interactions as described by Equation (1).

$$U_{\text{nonbonded}} = 4\epsilon \left[\left(\frac{\sigma}{r} \right)^{12} - \left(\frac{\sigma}{r} \right)^6 \right] + \frac{q_i q_j}{4\pi \epsilon_0 r} \quad (1)$$

$$U_{\text{bonded}} = U_{\text{bond}} + U_{\text{angle}} + U_{\text{dihedral}} \quad (2)$$

$$U_{\text{bond}} = K_{\text{bond}}(r - r_0)^2 \quad (3)$$

$$U_{\text{angle}} = K_{\text{angle}}(\theta - \theta_0)^2 \quad (4)$$

$$\text{Harmonic dihedral} : U_{\text{dihedral}} = K_{\text{dihedral}} [1 + d \cos(n\phi)] \quad (5)$$

$$\text{Multi harmonic dihedral} : U_{\text{dihedral}} = \sum_{n=1,5} A_n \cos^{n-1}(\phi) \quad (6)$$

where ϵ , σ , r , q_i , q_j and ϵ_0 are the energy well depth, closest distance of approach, distance between the two particles, charges on particle i and j and permittivity of free space, respectively. All the nonbonded interaction parameters are given in Table 1. The bonded interactions

Table 1. Nonbonded force field parameters used in this work.

Atoms/groups	ϵ (kcal/mol)	σ (Å)	q (e)
Water [30]			
O	0.155	3.166	−0.8476
H	0.000	0.000	0.4238
$C_{12}E_3$ [32]			
CH_3 (in alkane)	0.175	3.905	0.0000
CH_2 (in alkane)	0.118	3.905	0.0000
CH_2 (in –O– CH_2 – CH_2 –)	0.118	3.905	0.2500
O (in –O– CH_2 – CH_2 –)	0.170	3.000	−0.5000
CH_2 (in – CH_2 –O–H)	0.118	3.905	0.2650
O (in –OH)	0.200	3.150	−0.7000
H (in –OH)	0.200	3.150	0.4350
Silica nanoparticle [33]			
Si	0.093	3.697	1.1000
O (bridging)	0.054	3.0914	−0.5500
O (in –OH)	0.122	3.0914	−0.6750
H (in –OH)	0.015	0.9666	0.4000
Si (in –SiO $^-$)	0.093	3.697	0.7250
O $^-$ (in –SiO $^-$)	0.122	3.0914	−0.9000
Na^+	0.094	2.824	1.0000
Hexadecane [31]			
CH_3	0.175	3.905	0.0000
CH_2	0.118	3.905	0.0000

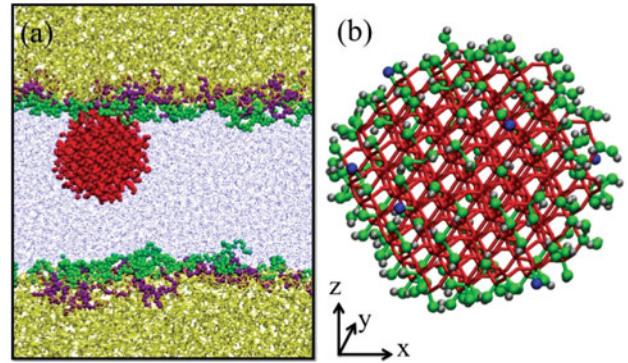


Figure 1. (a) Snapshot showing the side view of a simulation box having oil–water NP and surfactants. The water is in the center with NP and hexadecane surrounds the water from top and bottom. Surfactant ($C_{12}E_3$) are present at the oil–water interfaces. (b) Atomistic representation of silica NP (DI = 0.2).

include bonds, angles and dihedrals as given in Equation (2). Contribution of each term in Equation (2) is described in Equations (3)–(6). r_0 and θ_0 are the equilibrium bond distance and equilibrium angle, respectively. In Equations (5) and (6) we have defined two different formulas for dihedral. All the dihedrals are defined using one of the two formulas as mentioned in Table 2. All the bonded force field parameters are given in Table 2.

The simulation box shown in Figure 1 is a rectangular parallelepiped in which the box length in the x and y directions (L_x and L_y) are kept fixed at 108 and 96 Å, respectively. The box consists of hexadecane and water phases along with the surfactant ($C_{12}E_3$) and silica NP. Two hexadecane–water interfaces are present in the

Table 2. Bonded force field parameters used in this work.

	Bonds				
	K_{bond} (kcal/(mol. Å ²))		r_0 (Å)		
Water [30]					
O–H	1000.0		1.0		
C ₁₂ E ₃ [32]					
CH ₂ /CH ₂ –CH ₂	620.0		1.54		
CH ₂ –O(H)	900.0		1.43		
CH ₂ –Os	600.0		1.41		
O–H	553.0		0.945		
Silica [33]					
O–H (silanol)	495.0		0.945		
Hexadecane [31]					
CH ₃ /CH ₂ –CH ₂	620.0		1.54		
	Angles				
	K_{angle} (kcal/(mol.rad ²))		θ_0 (deg)		
Water [30]					
H–O–H	1000.0		109.47		
C ₁₂ E ₃ [32]					
CH ₂ –O–H	55.085		108.5		
CH ₂ –Os–CH ₂	62.09		112.0		
CH ₂ –CH ₂ –OH	62.09		108.0		
CH ₂ –CH ₂ –CH ₂	62.09		114.0		
CH ₂ –CH ₂ –Os	62.09		112.0		
Silica [33]					
Si–O–H	50.00		115.0		
Hexadecane [31]					
CH ₃ /CH ₂ –CH ₂ –CH ₂	62.09		114.0		
	Dihedrals				
Multi harmonic					
(kcal/mol)	A_1	A_2	A_3	A_4	A_5
CH ₂ –CH ₂ –O–H	0.6744	0.70339	0.1160	–1.4940	0.0
CH ₂ –CH ₂ –CH ₂ –CH ₂	2.0069	4.01180	0.2710	–6.2896	0.0
Harmonic					
	K_{dihedral} (kcal/mol)		d		n
CH ₂ –CH ₂ –Os–CH ₂	0.75		1		3
CH ₂ –CH ₂ –CH ₂ –Os	1.0		1		3

system. We have considered our system to consist of 15,000 water molecules, 1000 hexadecane molecules, 100 C₁₂E₃ molecules and 1 silica NP. The silica NP is considered as a rigid body during simulation, except that the H atom of –SiOH group on its surface is flexible. Periodic boundary conditions are applied in all the directions. Simulations are performed to study the effect of changing DI of silica NP. DI values of 0.0, 0.1, 0.2, 0.5 and 1.0 have been used in the simulations. DI value of 0.5 means that 0.5 –SiOH (silanol) groups on surface of silica NP are

ionised to –SiO[–] per nm² surface area of NP and DI = 0.0 means unionised NP (0.0 silanol groups are ionised). These DI values are taken based on the experimental data corresponding to different pH values [33]. All the systems simulated are identical except that the DIs of NP used in different systems is changing.

All the simulations are performed using LAMMPS package [35]. Long-range electrostatic interactions are accounted using particle particle particle mesh technique as implemented in LAMMPS package. A cut-off distance of 1.2 nm is used for the nonbonded interactions and a time step of 1.0 fs is used. The simulations are performed using NPTA ensemble where the number of particles, pressure, temperature and area of the interface are kept constant during the simulations. The velocity-Verlet algorithm is used for integrating the equations of motion. The temperature is maintained at 300 K and pressure at 1 atm using the Nose–Hoover thermostat and barostat with the damping parameters of 0.1 and 1.0 ps, respectively. The box length in the z direction fluctuates to maintain the equilibrium density of different phases present in the system and is done by applying the barostat only in the z direction. The total simulation time is 20 ns. All the snapshots are generated using Visual Molecular Dynamics (VMD) [36] program.

3. Results and discussions

To quantify the effect of changing DI of silica NP, we have considered five different DI (0.0, 0.1, 0.2, 0.5 and 1.0) values of silica NP. A silica NP is considered in hexadecane–water system along with C₁₂E₃ nonionic surfactants. Figure 2 shows the snapshots of the systems having NP with different DI. It is evident from Figure 2(a–e) that as the DI increases, the NP shifts from the hexadecane–water interface to the bulk water. The shift of the NP towards the bulk water is due to the increasing hydrophilic nature of silica NP with increase in the DI value. Figure 2(f) shows the top view of Figure 2(a),

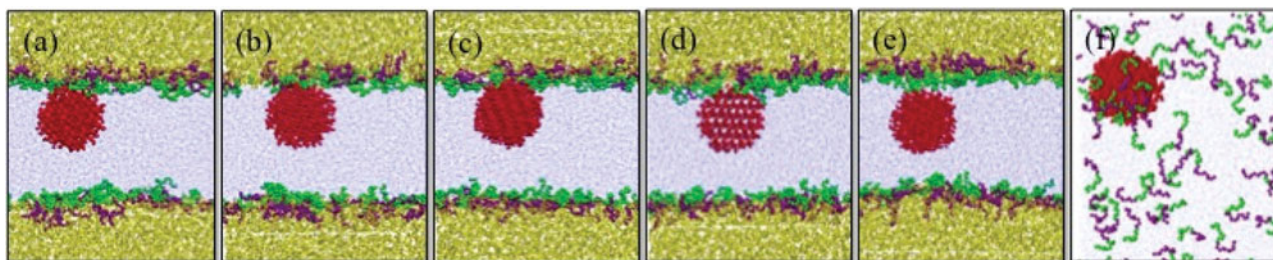


Figure 2. Snapshots showing the side view of oil–water NP and surfactant system. The water is in the center with NP and hexadecane surrounds the water from top and bottom. Surfactant (C₁₂E₃) are present at the oil–water interfaces. The NPs have different DI (a) 0.0, (b) 0.1, (c) 0.2, (d) 0.5, (e) 1.0 –OH groups ionised per nm² surface area of NP and (f) The top view of (a) from oil phase.

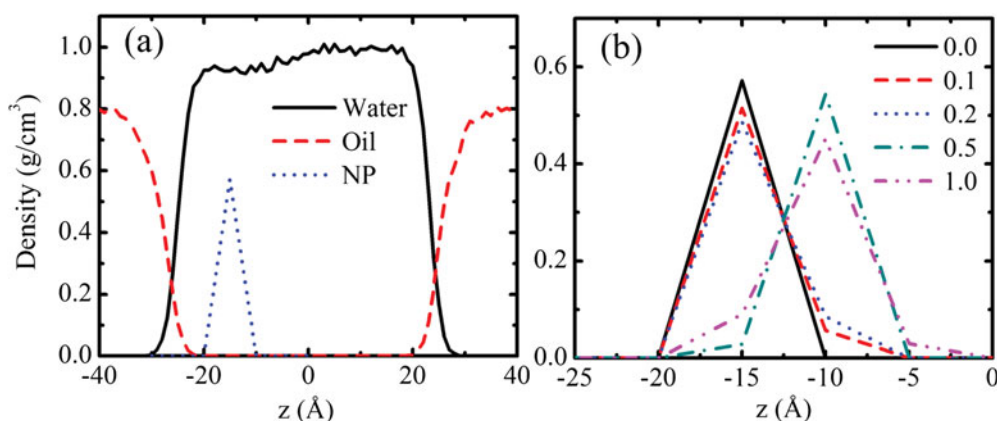


Figure 3. (a) Density profile (ρ) of water, oil and NP for unionised silica (DI = 0.0) NP system. (b) Density profile of silica NP with different DI. Different types of line represent various DI of NP.

from the oil phase (oil molecules have been removed for clarity). The surfactant molecules are found to disperse throughout the interface with slightly more concentration close to NP due to adsorption.

The observations from the snapshots in Figure 2 is further verified by calculating the density profiles of various components present in the system, along the z direction for different planes of width $\Delta z = 5 \text{ \AA}$ parallel to the hexadecane–water interface. Figure 3(a) shows the density profile of oil, water and NP system at DI = 0.0. The NP remains in the water phase but stays close to the oil–water interface. It should be noted that the system contains only one NP, thus the NP stays close to any one of the interfaces. The position of NP states that the NP is hydrophilic in nature. Changing the DI of silica NP has an effect on the NP location with respect to the interface. As the DI increases, NP shifts more towards the water phase. Figure 3(b) shows the density profiles of NP with different DIs, calculated using the position of centre of mass of the NP. $z = 0$ on the x axis in Figure 3 represents the centre of the water phase. It should be noted that the number of configurations considered for obtaining the density profiles are limited and thus the profiles may have non-negligible error. Thus, here the intention of the density profile is to indicate the NP position with respect to the interface. It is evident from the density profile that increasing DI shifts the particle toward the centre of water phase, i.e. away from the interface. NP stays near the interface for DI values of 0.0, 0.1 and 0.2. For higher DI values of 0.5 and 1.0 the density profile peak shifts away from the interface towards the water centre. This is a clear indication that the NP becomes more hydrophilic with the increasing DI. Similar case has already been observed in the literature for the case of graphene oxide (GO) where decreasing pH makes the GO less hydrophilic and thus allowing it to move to the oil–water interface [29].

In order to study the adsorption of $C_{12}E_3$ on the surface of silica NP with changing DI, we have calculated the number density (ρ_s) of the oxygen atoms (Os) of ether group of $C_{12}E_3$ around the silica NP using the expression: $\rho_s = \frac{\langle N(r, r + \Delta r) \rangle}{4\pi r^2 \Delta r}$. Here $\langle N(r, r + \Delta r) \rangle$ is the average number of oxygen atoms (Os) in a spherical shell between distance r and $(r + \Delta r)$ from the silanol group (O and H atoms) of a silica NP. Figure 4 shows the number density calculated with respect to O and H atoms of the $-\text{SiOH}$ groups, respectively. As the DI increases, the peak height of the number density decreases and finally the peak vanishes, although the peak position remains the same for all the DI values, at 2.75 and 1.85 Å for O and H atoms of $-\text{SiOH}$ group, respectively. This behaviour of number density with increasing DI suggests that there is a decrease in the adsorption of surfactants on the NP. The maximum adsorption is observed for unionised NP, and as the NP is ionised the adsorption of surfactant on NP is found to reduce. Strong adsorption is seen for DI < 0.2, while depletion behaviour is observed for higher DI values. The depletion effect for DI = 0.5 and 1.0 in Figure 4 is due to the increasing hydrophilic nature of the silica NP due to which NP shifts from the interface to the bulk water. On the other hand, the surfactant prefers to stay at the interface causing the depletion effect at higher DI values.

Although the total amount of adsorption is not very high, if we compare qualitatively then there is a decrease in adsorption with the increasing DI. Studies have reported that the cause for the adsorption is the formation of hydrogen bonds between silica and nonionic surfactant [37]. In order to understand the behaviour observed in this work, we also calculate the number of hydrogen bonds formed by the NP with the surfactants. The number of hydrogen bonds formed for different DI of NP is shown in Figure 5(a). The criteria [38] followed for identifying the formed hydrogen bond include that

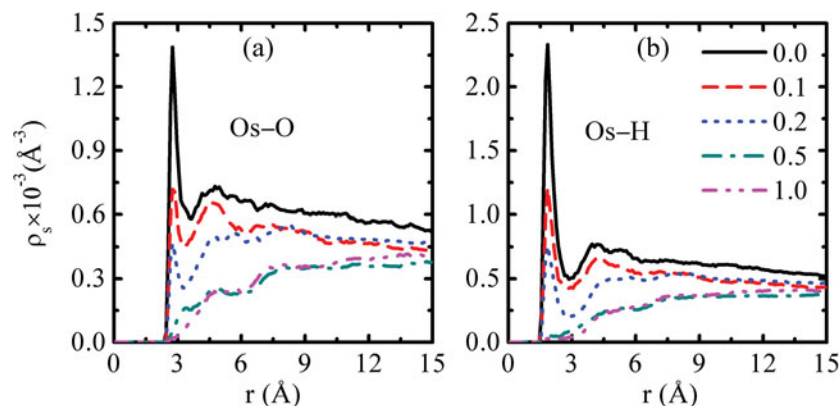


Figure 4. Number density (ρ_s) of oxygen atoms of ether group (Os) of surfactant ($C_{12}E_3$) with respect to O and H atoms of silanol groups of silica NP, respectively, in panels a and b.

the distance between the two oxygen atoms of silanol group and surfactant, $R_{OO} < 3.5 \text{\AA}$ and the angle formed by the $-\text{OH}$ group and the oxygen atom of the other molecule, $\text{HO}\cdots\text{O}$ angle $< 30^\circ$. The criteria for the distance $R_{OO} < 3.5 \text{\AA}$ is obtained from the number density plot in Figure 4(a), where the minimum of the first peak is obtained close to 3.5\AA . We have counted the total number of hydrogen bonds formed between a silica NP and surfactants by calculating the hydrogen bond formed by the silanol group of silica NP with both the ether oxygen and terminal OH group of $C_{12}E_3$ molecule. It is found that as the DI increases the number of hydrogen bonds formed between the NP and the surfactant decreases. For $\text{DI} \geq 0.5$ the number of hydrogen bonds formed are close to zero. Thus, the amount of adsorption of surfactant on the NP surfaces increases with increase in the formation of hydrogen bonds between the silica NP and surfactant molecules.

To further support our observation we have counted the total number of oxygen atoms of $C_{12}E_3$ within the

distance $< 3.5 \text{\AA}$ from the O atom of $-\text{SiOH}$, which is shown in Figure 5(b). The number shows the same trend as hydrogen bonds. Decreasing DI increases the number of oxygen atoms adsorbed on the NP surface. Based on the above results, it is clear that decreasing DI of silica NP increases the amount of adsorption of $C_{12}E_3$ surfactants. The reason for the change in the number of hydrogen bonds formed with the changing DI is shown in Figure 6 with the help of the cartoon. The cartoon shows that with increasing pH the DI of NP increases, which converts $-\text{SiOH}$ groups on the surface of silica NPs to $-\text{SiO}^-$ making them incapable to form hydrogen bonds with the oxygen (Os) of the ether group of surfactant. Part (b) of the cartoon shows that at high pH there are very less number of $-\text{SiOH}$ groups leading to negligible adsorption of surfactant due to hydrogen bonding, while at low pH there are large number of $-\text{SiOH}$ groups on NP surface and thus surfactant molecules adsorb on them due to the formation of hydrogen bonds.

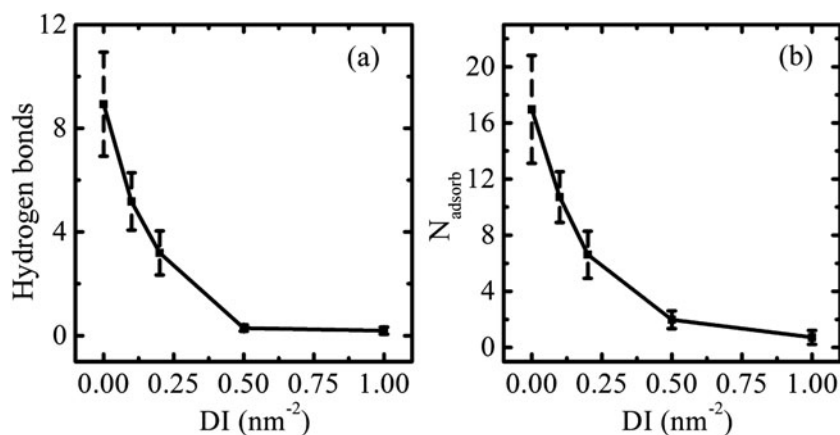


Figure 5. (a) Number of hydrogen bonds formed by a NP with the changing DI of silica NP. (b) Number of oxygen atoms of $C_{12}E_3$ surrounding the silica NP with the changing DI of silica NP.

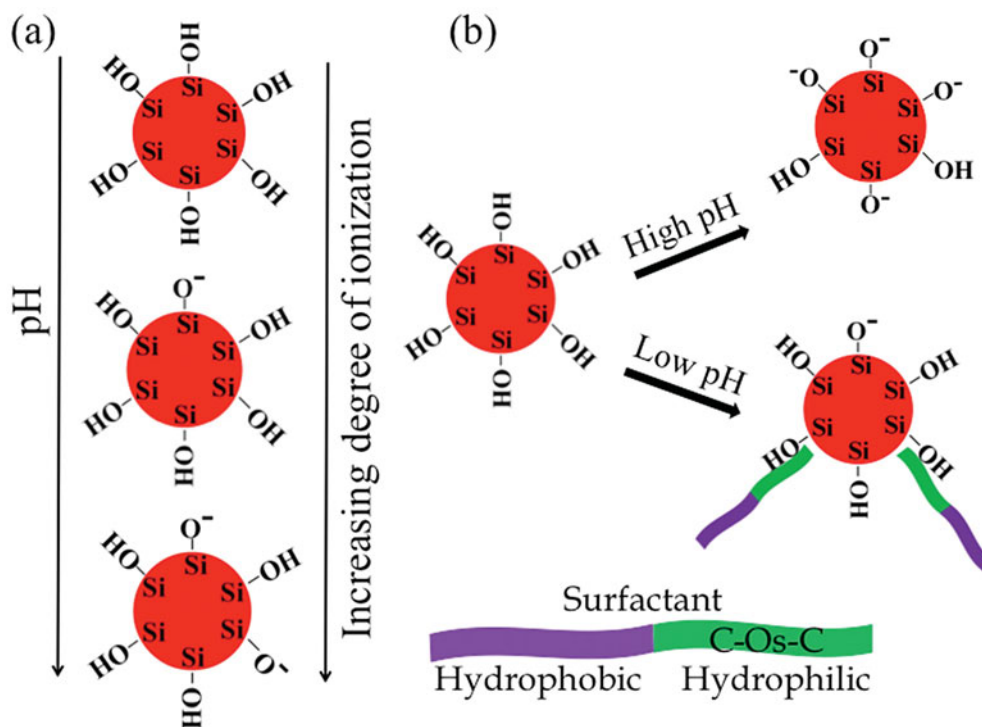


Figure 6. (a) The cartoon showing the qualitative representation of different DI of silica NP and (b) the mechanism of adsorption of surfactant on the NP surface. The surfactant molecule is represented by a ribbon structure.

The behaviour of the surfactants in the presence of NP with changing DI can also be explained with the help of potential of mean force (PMF) calculation. The PMF is calculated using the following expression: $PMF = -k_B T \ln(p(r))$ [39], where $p(r)$ is the ratio of the number density of a particular atom, in this case oxygen of the ether group of $C_{12}E_3$ (Os), divided by its number density in the bulk. Figure 7 shows the PMF values as a function of distance for varying DI values. For high values of DI such as 0.5 and 1.0 there is no energy well observed in the PMF profile, and with the increase in distance the PMF reaches a constant value. In the case of lower DI values, i.e. 0.0, 0.1 and 0.2 the energy wells are observed. The energy wells are obtained at same distances close to 2.75 Å and 1.85 Å for Os–O and Os–H, respectively, for all the DI values. As the DI decreases the well depth of the PMF increases resulting in an increased affinity between the surfactants and silanol groups of silica NP. This leads to an increase in adsorption of surfactant molecule on the silica NP with decreasing DI.

We have earlier asserted that the change in the IFT is due to the change in the DI of silica NPs. In order to confirm the same, we also calculate the IFT for the oil–water systems containing silica NP with varying DI. The results obtained did not show any change in the IFT values with the changing DI values, as shown in Figure 8. This we

believe is due to the fact that there is only one NP in the system and so its effect on the IFT is not noticeable. In a recent work of Sinha *et al.* [40], it was shown that at small volume fractions (less than 7%) of NPs the surface tension values of water remain unchanged. The volume fraction corresponding to one silica NP used in this study is $\sim 3\%$. We believe that, based on the current results, for a system with a significant number of NPs, we may obtain results as observed in the coarse-grained simulations and experiments [23,24].

Nevertheless, in order to further probe the effect of the presence of NP on the system, we also plot the energy profile across the interfacial region in Figure 9(a) and the corresponding density profile in Figure 9(b). The energy and density profiles are obtained along the z direction for different planes of width, $\Delta z = 1$ Å, parallel to the hexadecane–water interface. $E_{\text{per particle}}$ is the total energy per atom in each plane. The dotted line at $z = -20$ Å marks the end of interfacial region of the interface containing both NP and surfactants. It is evident from the energy profile at the interface close to $z = -20$ Å that as the DI increases the magnitude of energy decreases. For lower DI values the magnitude of energy is more and so the energy required to increase the interfacial area by unity should be more, as compared to higher DI values. Thus, we can infer that the system having NP with lower

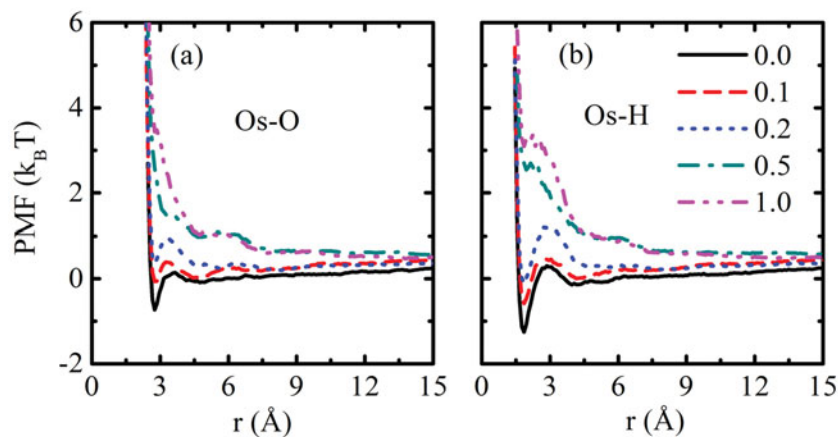


Figure 7. PMF of ether group (Os) of surfactant ($C_{12}E_3$) with respect to O atom (a) and H atom (b) of silanol groups of silica NP, respectively.

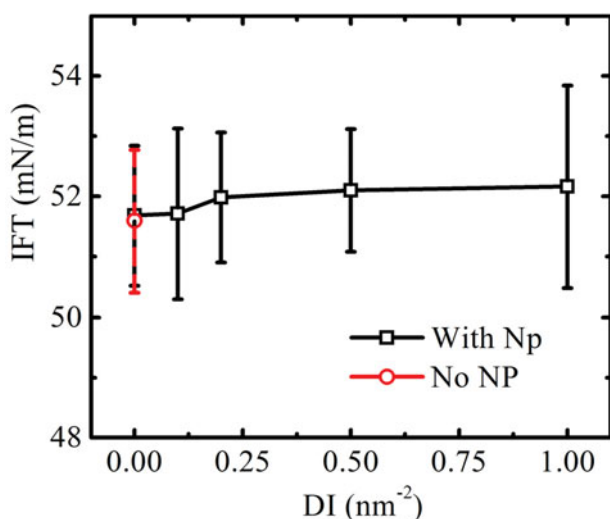


Figure 8. Variation of IFT of oil-water, NP and surfactant ($C_{12}E_3$) system with the changing DI of silica NP.

DI should have high IFT value as compared to high DI values. However, in our study we did not observe any such change in IFT that is due to very small change in energy, which is insufficient to show its effect on the IFT. It should be noted that $E_{\text{per particle}}$ hardly changes with DI at the other interface, containing only surfactant, present in the system between 20\AA to 30\AA in the z direction.

We would also like to mention that the surfactant, $C_{12}E_3$, considered in this work has a very small length of hydrophilic chain. It is likely that increasing the chain length will vary the adsorption behaviour. Also, the size of the NP considered in simulations is very small (diameter = 3 nm), and as per Bharti *et al.*, increasing the NP size will increase the amount of adsorption [16]. Thus, changing parameters such as surfactant chain length and NP size will result in the change in amount of adsorption.

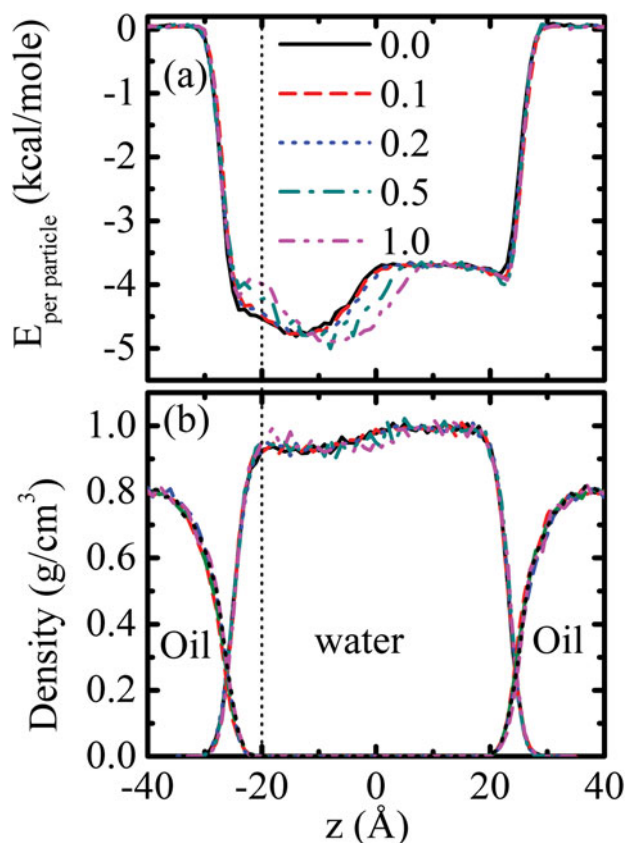


Figure 9. (a) Energy profile for hexadecane-water, NP and surfactant ($C_{12}E_3$) system with the changing DI of silica NP. (b) Density profile of water and oil for different DI of silica NP. Solid lines represent the density of water and dashed lines represent density of oil. The colour codes are same for both (a) and (b).

In our previous work [23], we have studied the effect of adsorption by using coarse grained molecular dynamics simulations using the MARTINI force field, where we studied the effect of adsorption by artificially tethering the surfactant molecules to the NPs surface. Using that model we could successfully show that when there is no

adsorption on the NPs there is no effect of adding NPs to the system, while if the surfactant molecules adsorb on the NPs then there is an increase in the oil–water IFT. The major drawback of that study was that the adsorption was done artificially. There was still a question that in reality if there is any adsorption or not, and if the adsorption occurs then how does it varies with the pH. From the current study we have illustrated that adsorption of non-ionic surfactant occurs on the surface of silica NP, which vary with the change in DI. At higher pH /DI, we observe negligible adsorption of surfactants on the NPs and as the pH /DI decreases the adsorption of surfactant on NP increases. This change in the adsorption phenomena is the cause for the different behaviours such as increase or no change in IFT on the addition of silica NPs to oil–water nonionic surfactant system as observed in the literature. Thus, this study fills the gap between our understanding and the experimentally observed results.

4. Conclusions

The adsorption of nonionic surfactant ($C_{12}E_3$) on the silica NP in hexadecane–water system is studied using an all atom molecular dynamic simulation. The adsorption of surfactant on the NP is observed to decrease with the increase in DI of silica NP. Adsorption is observed to occur due to the formation of hydrogen bonds between the silica NP and the surfactant molecules. Increasing DI leads to a reduction in the number of hydrogen bonds formed due to the decrease in the availability of the silanol groups on the NP. The PMF also shows an increase in the affinity to adsorb with decrease in the DI. The energy profile shows the decreasing magnitude of energy at the interface with increasing DI. In experiments pH is responsible for the change in DI of the silica NPs. This study explains that at low pH there is adsorption of nonionic surfactant on the silica NP surface and as the pH increases the adsorption reduces.

Acknowledgments

This work is supported by the Department of Science and Technology (DST), Government of India. The computational resources are provided by the HPC cluster of the Computer Center (CC), Indian Institute of Technology Kanpur.

Disclosure statement

No potential conflict of interest was reported by the authors.

Funding

Science and Engineering Research Board [grant number SB/S3/CE/079/2015]

References

- [1] N.R. Tummala, L. Shi, and A. Striolo, *J. Colloid Interface Sci.* **362**, 135 (2011). doi:10.1016/j.jcis.2011.06.033.
- [2] A. Thibaut, A.M. Misselyn-Bauduin, J. Grandjean, G. Broze, and R. Jérôme, *Langmuir* **16**(24), 9192 (2000). doi:10.1021/la000302e.
- [3] M. Dracha, L. Łajtara, J. Narkiewicz-Michałka, W. Rudzińska, and J. Zajc, *Colloids Surf. A* **145**(1), 243 (1998). doi:10.1016/S0927-7757(98)00676-1.
- [4] S. Thomas, *Oil Gas Sci Technol – Rev. IFP* **63**(1), 9 (2008). doi:10.2516/ogst:2007060.
- [5] R. Zhang and P. Somasundaran, *Adv. Colloid Interface Sci.* **123**, 213 (2006). doi:10.1016/j.cis.2006.07.004.
- [6] B.K. Pilapil, H. Jahandideh, S.L. Bryant, and M. Trifkovic, *Langmuir* **32**(28), 7109 (2016). doi:10.1021/acs.langmuir.6b00873.
- [7] P. Li and M. Ishiguro, *Soil Sci. Plant Nutr.* **62**(3), 223 (2016). doi:10.1080/00380768.2016.1191969.
- [8] K.P. Sharma, V.K. Aswal, and G. Kumaraswamy, *J. Phys. Chem. B* **114**(34), 10986 (2010). doi:10.1021/jp1033799.
- [9] S. Partyka, S. Zaini, M. Lindheimer, and B. Brun, *Colloid Surf.* **12**, 255 (1984). doi:10.1016/0166-6622(84)80104-3.
- [10] P. Somasundaran, E.D. Snell, and Q. Xu, *J. Colloid Interface Sci.* **144**(1), 165 (1991). doi:10.1016/0021-9797(91)90247-6.
- [11] S.C. Biswas and D.K. Chattoraj, *J. Colloid Interface Sci.* **205**(1), 12 (1998); T.P. Goloub, L.K. Koopal, B.H. Bijsterbosch, and M.P. Sidorova, *Langmuir* **12** (13), 3188 (1996).
- [12] T.V.D. Boomgaard, T.F. Tadros, and J. Lyklema, *J. Colloid Interface Sci.* **116**(1), 8 (1987). doi:10.1016/0021-9797(87)90091-9.
- [13] R. Denoyel and J. Rouquerol, *J. Colloid Interface Sci.* **143**(2), 555 (1991). doi:10.1016/0021-9797(91)90287-1.
- [14] B.R. Postmus, F.A.M. Leermakers, L.K. Koopal, and M.A. Cohen Stuart, *Langmuir* **23**(10), 5532 (2007). doi:10.1021/la063525z.
- [15] S.K. Singh and S.M. Notley, *J. Phys. Chem. B* **114**(46), 14977 (2010). doi:10.1021/jp107224r.
- [16] B. Bharti, J. Meissner, U. Gasser, and G.H. Findenegg, *Soft Matter* **8**(24), 6573 (2012). doi:10.1039/c2sm25648g.
- [17] P.G. Cummins, E. Staples, and J. Penfold, *J. Phys. Chem.* **94**(9), 3740 (1990). doi:10.1021/j100372a071.
- [18] J. Penfold, E. Staples, I. Tucker, and P. Cummins, *J. Phys. Chem.* **100**(46), 18133 (1996). doi:10.1021/jp9611838.
- [19] G. Despert and J. Oberdisse, *Langmuir* **19**(18), 7604 (2003). doi:10.1021/la0300939.
- [20] D. Lugo, J. Oberdisse, M. Karg, R. Schweins, and G.H. Findenegg, *Soft Matter* **5**(15), 2928 (2009). doi:10.1039/b903024g.
- [21] D.M. Lugo, J. Oberdisse, A. Lapp, and G.H. Findenegg, *J. Phys. Chem. B* **114**(12), 4183 (2010). doi:10.1021/jp911400j.
- [22] S. Paria and K.C. Khilar, *Adv. Colloid Interface Sci.* **110**(3), 75 (2004). doi:10.1016/j.cis.2004.03.001.
- [23] P. Katiyar and J.K. Singh, *J. Chem. Phys.* **146**(20), 204702 (2017). doi:10.1063/1.4984073.
- [24] N.R. Biswal, N. Rangera, and J.K. Singh, *J. Phys. Chem. B* **120**, 7265 (2016); N.R. Biswal and J.K. Singh, *RSC Adv.* **6**, 113307 (2016).

- [25] R. Pichot, F. Spyropoulos, and I.T. Norton, *J. Colloid Interface Sci.* **377**, 396 (2012). doi:10.1016/j.jcis.2012.01.065.
- [26] H. Ma, M. Luo, and L.L. Dai, *Phys. Chem. Chem. Phys.* **10**, 2207 (2008). doi:10.1039/b718427c.
- [27] E.J. Burcik and C.R. Vaughn, *J. Colloid Sci.* **6**, 522 (1951). doi:10.1016/0095-8522(51)90050-5.
- [28] J. Permpasert and S. Devahastin, *J. Food Eng.* **70**(2), 219 (2005). doi:10.1016/j.jfoodeng.2004.08.045.
- [29] J. Kim, L.J. Cote, F. Kim, W. Yuan, K.R. Shull, and J. Huang, *J. Am. Chem. Soc.* **132**, 8180 (2010). doi:10.1021/ja102777p.
- [30] H.J.C. Berendsen, J.R. Grigera, and T.P. Straatsma, *J. Phys. Chem.* **91**(24), 6269 (1987). doi:10.1021/j100308a038.
- [31] E.K. Boland, J. Liu, and J.K. Maranas, *J. Chem. Phys.* **132**(14), 144901 (2010). doi:10.1063/1.3366660.
- [32] L. Shi, N.R. Tummala, and A. Striolo, *Langmuir* **26**, 5462 (2010).
- [33] F.S. Emami, V. Puddu, R.J. Berry, V. Varshney, S.V. Patwardhan, C.C. Perry, and H. Heinz, *Chem. Mater.* **26**, 2647 (2014). doi:10.1021/cm500365c.
- [34] H. Fan, D.E. Resasco, and A. Striolo, *Langmuir* **27**, 5264 (2011). doi:10.1021/la200428r.
- [35] S.J. Plimpton, *J. Comp. Phys.* **117**, 1 (1995). doi:10.1006/jcph.1995.1039.
- [36] W. Humphrey, A. Dalke, and K. Schulten, *J. Mol. Graph.* **14**, 33 (1996). doi:10.1016/0263-7855(96)00018-5.
- [37] J. Penfold, E. Staples, and I. Tucker, *Langmuir* **18**, 2967 (2002). doi:10.1021/la011575s.
- [38] D. Roy, S. Liu, B.L. Woods, A.R. Siler, J.T. Fourkas, J.D. Weeks, and R.A. Walker, J.J. Karnes, E.A. Gobrogge, R.A. Walker, and I. Benjamin, *J. Phys. Chem. C* **117**(51), 27052 (2013), *J. Phys. Chem. B* **120** (8), 1569 (2016).
- [39] K. Anitha, S. Namsani, and J.K. Singh, T. Mendez-Morales, J. Carrete, M. Perez-Rodriguez, O. Cabeza, L.J. Gallego, R.M. Lynden-Bell, and L.M. Varela, P. Katiyar, T.K. Patra, J.K. Singh, D. Sarkar, and A. Pramanik, *J. Phys. Chem. A* **119**(30), 8349 (2015), *Phys. Chem. Chem. Phys.* **16** (26), 13271 (2014), *Chem. Eng. Sci.* **141**, 293 (2016).
- [40] N. Sinha and J.K. Singh, *J. Mol. Liq.* **246**, 244 (2017). doi:10.1016/j.molliq.2017.09.059.